Available online at www.sciencedirect.com
ScienceDirect
Journal of Sound and Vibration 319 (2009) 247–259
JOURNAL OF SOUND AND VIBRATION
www.elsevier.com/locate/jsvi

Dominant frequencies of train-induced vibrations

Shen-Haw Ju*, Hung-Ta Lin, Jeng-Yuan Huang

Department of Civil Engineering, National Cheng-Kung University, Ta-Hsueh Road, Tainan 70101, Taiwan

Received 3 April 2007; received in revised form 13 March 2008; accepted 17 May 2008
Handling Editor: L.G. Tham
Available online 1 July 2008

Abstract

This paper investigates the dynamic characteristics of ground vibrations induced by moving vehicles including the mass rapid transit system, high-speed train railway, and general railway on bridges, embankments, and in tunnels using field experiments and theoretical solutions. The results indicate that train-induced ground vibrations at the trainload dominant frequencies are significantly large for both subsonic and supersonic train speeds, and the vibrations from carriage natural frequencies and engine frequencies are minor. For trains moving on bridges, the resonant vibrations are serious when the natural frequencies of the bridge are close to the trainload dominant frequencies, but resonance does not occur when the carriage natural frequencies and trainload dominant frequencies match. The trainload dominant frequency and its influence factor can be computed using the two simple equations deducted in this paper.

1. Introduction

Mass rapid transit (MRT) systems and high-speed trains often produce significant ground vibrations; thus, understanding the vibration characteristics induced by trains has become an important issue. Li and Su [1] investigated the fundamental characteristics and the influential factors of the resonant vibrations of a girder bridge under high-speed trains. They indicated that the number of vehicles passing the bridge is an important factor. If the number of vehicles is small, resonance may not occur. Wang et al. [2] studied the applicability of passive tuned mass dampers (PTMDS) to suppress train-induced vibrations on bridges. They pointed out that PTMD have good control efficiency only when the train travels at resonant speed. Yang et al. [3] used the condition of resonance and cancellation for the waves generated by continuously moving loads on a beam, and proposed the optimal design criteria that are effective for suppressing the resonant response. Ju [4] used the three-dimensional finite element method to simulate soil vibrations due to a moving high-speed train passing a bridge system, and suggested that the train could operate with reasonable velocity and avoid resonance. Wu and Yang [5] presented a procedure for analyzing the vehicle–rails–bridge system, by which the dynamic response of each subsystem can be computed. They identified the maximum response of the train caused by the train–rail–bridge resonance. Xia et al. [6] investigated the resonance mechanism and conditions of a train–bridge system using theoretical derivations, numerical simulations, and experimental data analyses.

*Corresponding author. Tel.: +886 6 2757575 63119; fax: +886 6 2358542.
E-mail address: juju@mail.ncku.edu.tw (S.-H. Ju).

0022-460X/$ - see front matter © 2008 Elsevier Ltd. All rights reserved.
doi:10.1016/j.jsv.2008.05.029

Ju and Lin [7] studied the vibration characteristics of a three-dimensional arch bridge when high-speed trains pass it. In their paper, two resonance criteria with simple formulae were advised to predict the resonance effect of the arch bridge and the high-speed train. Ju and Lin [8] investigated the resonant vibration characteristics of a three-dimensional vehicle–bridge system when high-speed trains pass bridges. In order to avoid resonance, they especially emphasized that the dominated train frequencies and the bridge natural frequencies should be as different as possible. Yau and Yang [9] developed a wideband tuned damper system for reducing the multiple resonant responses of continuous truss bridges to moving trainloads. Ju [10] used finite element analyses to investigate the behavior of building vibrations induced by high-speed trains moving on bridges. Finite element results indicated that trainload frequencies were more important than the natural frequencies of bridges and trains for building vibrations. Yang et al. [11] studied the mechanisms underlying the resonance and cancellation phenomena of an elastically supported bridge caused by a sequence of equidistant moving loads. Yau and Yang [12] studied the acceleration response of a simple beam subjected to successive moving loads with identical intervals. When the loads were moving at resonant speeds, the higher modes had significant influence on the acceleration amplitude. Ju and Lin [13] were the first to indicate that the dominant frequencies of the trainload are also significant when moving trains pass a free field using the numerical analysis. Ju et al. [14] proposed a field experiment to investigate the characteristics of the ground vibrations induced by a high-speed train traveling on a bridge, and the experimental results indicated that the vibration at the dominant frequencies of the trainload is significantly large.

Most of the above investigations were focused on the resonance mechanism and conditions of the vehicle–bridge interaction system. However, little effort has been oriented towards the investigation of the characteristics of the dominant vibration induced by moving trains. Therefore, this paper uses filed experiments and theoretical solutions to study the pattern of ground vibrations induced by trains moving on bridges, embankments, or in tunnels.

2. Dominant frequencies of a trainload

The trainload is an important source of induced vibrations, so its dominant frequencies should be known first. To evaluate them, the wheel loading of a train passing a point is assumed to be given by

$$P(t)=\sum_{j=1}^{N_c}\sum_{k=1}^{N_w}P_{\text{axle}}(\delta(t-t_k-jt_c)) \tag{1}$$

where the train has N_c carriages, a carriage has N_w pairs of wheels, P_{axle} is the load of a pair of wheels, δ is the unit impulse function, $t_k=s_k/V$, in which V is the train speed and s_k is the distance between the kth wheel and the beginning of the carriage, and $t_c=L/V$, in which L is the distance between two carriage centers. The Fourier transfer can be applied to Eq. (1) to convert the trainload function into the frequency domain as

$$P(f)=\int_{-\infty}^{\infty}P(t)\mathrm{e}^{-\mathrm{i}2\pi f}\,\mathrm{d}t=\sum_{j=1}^{N_c}\sum_{k=1}^{N_w}P_{\text{axle}}\mathrm{e}^{-\mathrm{i}2\pi f(t_k+jt_c)}=\sum_{j=1}^{N_c}\sum_{k=1}^{N_w}P_{\text{axle}}\mathrm{e}^{-\mathrm{i}2\pi f(s_k+jL)/V} \tag{2}$$

and $P(t)=\int_{-\infty}^{\infty}P(f)\mathrm{e}^{2\pi fti}\,\mathrm{d}f$.

The influence factors R_f can be determined by

$$R_f=\left|P(f)\right|=\left|\sum_{j=1}^{N_c}\sum_{k=1}^{N_w}P_{\text{axle}}\mathrm{e}^{-\mathrm{i}2\pi f(s_k+jL)/V}\right| \tag{3}$$

The dominant frequencies are defined as the relatively largest values of R_f, but they cannot be derived directly from Eq. (3). If $f\times t_c$ of Eq. (2) is a positive integer (n), or

$$f=n/t_c=nV/L, \tag{4}$$

Eq. (3) is changed to the sum of N_c carriage loads by

$$R_{f=nV/L} = N_c P_{\text{axle}} \left| \sum_{k=1}^{N_w} e^{-i2n\pi S_k/L} \right| \tag{5}$$

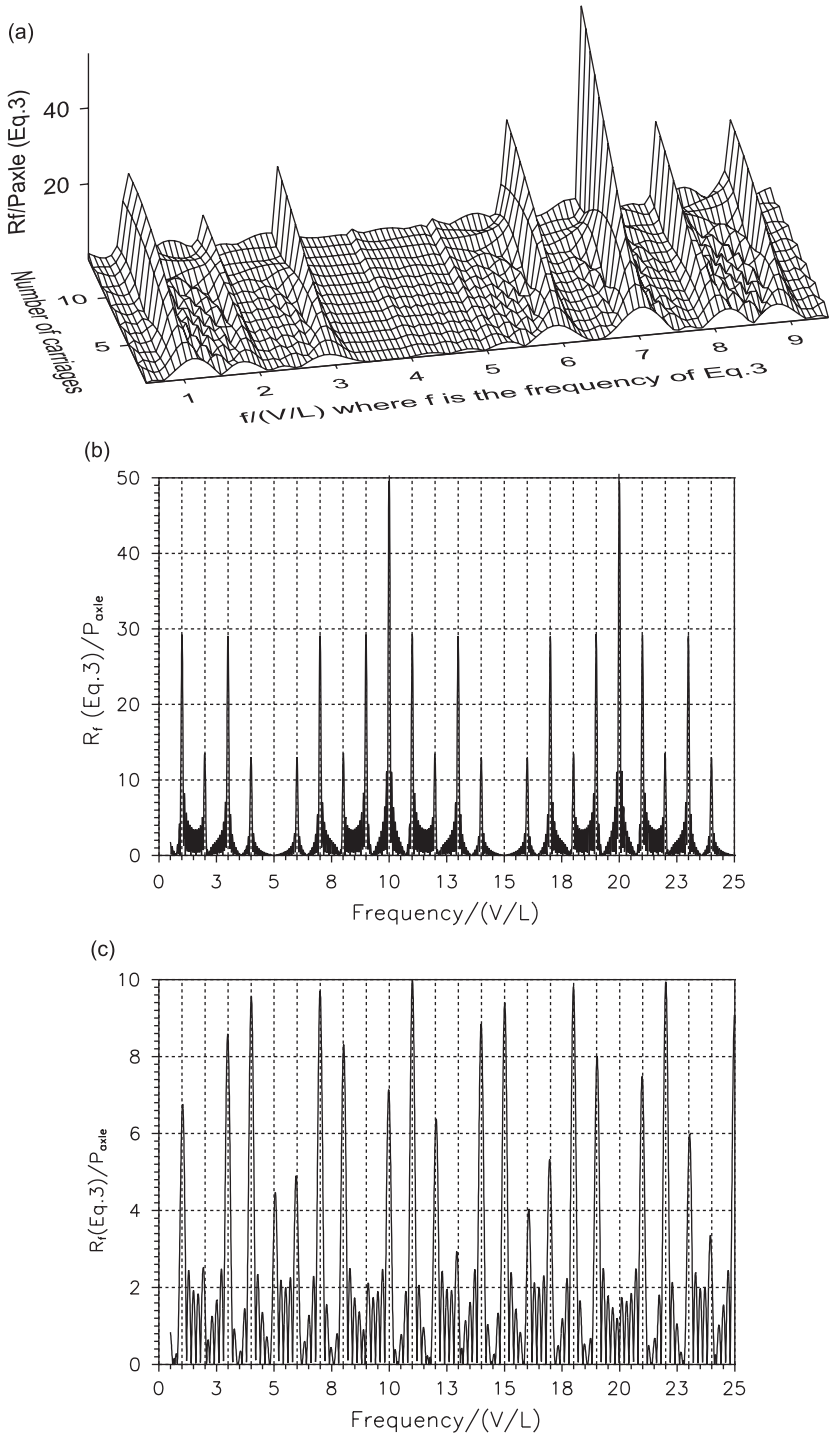

Fig. 1. R_f changing with theoretical trainload frequencies obtained from Eq. (3). (a) Taiwan railway train (1 to 14 carriages), (b) HSR-700T high-speed train (12 carriages), (c) Taipei MRT train (4 carriages).

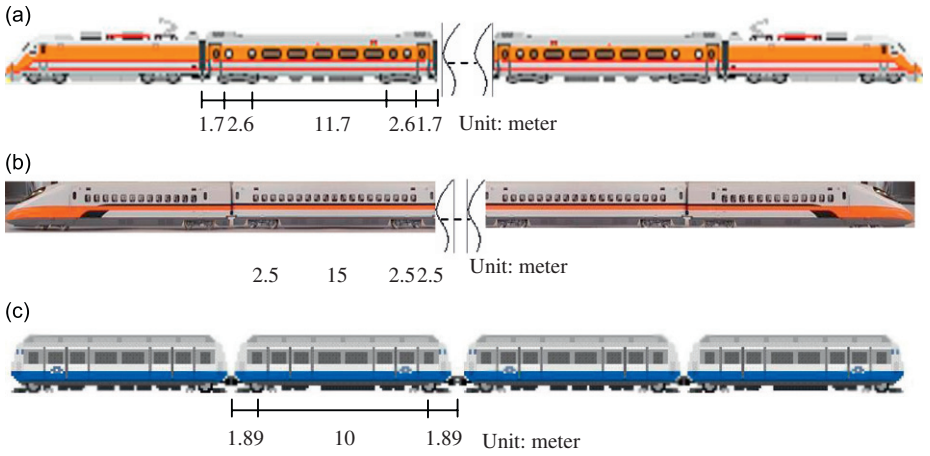

Fig. 2. Train dimensions used in the experiments of this study. (a) Taiwan railway train (Carriage interval = 20.3 m, 14 carriages), (b) HSR-700T high-speed train (Carriage interval = 25 m, 12 carriages), (c) Taipei MRT train (Carriage interval = 13.78 m, 4 carriages).

Otherwise, R_f can be canceled by each other due to the positive or negative sign of the load in the exponential function. Thus, if N_c is large enough, the frequencies of Eq. (5) should be the dominant frequencies of the trainload. Fig. 1(a) shows R_f using Eq. (3) for the Taiwan railway train as illustrated in Fig. 2(a), in which the number of carriages is set from 1 to 14. This figure indicates that the dominant frequencies can be precisely predicted as shown in Eq. (4) when the number of carriages is larger than 3. Eqs. (4) and (5) can be used to evaluate dominant frequencies and influence factors. The dominant frequencies are only dependent on the ratio of the train speed to the carriage length, and the influence factors are only dependent on the ratio of wheel locations to the carriage length, but independent of the train speed. Figs. 1(b) and (c) show R_f using Eq. (3) for the HSR-700T high-speed train and Taipei MRT train as illustrated in Figs. 2(b) and (c), respectively. These figures further validate the accuracy of Eq. (4).

3. Explanation of experimental and theoretical validation schemes

The dominant frequencies and influence factors derived in Section 2 will be validated using experimental and theoretical simulations. This section explains these schemes as follows:

3.1. Illustration of experiments

The field experiment contained vibration observation stations near the railroad. Since vibrations, presented as velocity, are often used in the international standard (such as the 1/3 octave band for the semi-conductor industry) vibration velocities were used to represent our experimental results. The setup and layout of the velocity meters are shown in Fig. 3, where the surface soil was removed to a depth of about 40 cm, and a 21 cm × 21 cm × 1 cm steel plate was fixed to the ground to hold the three velocity meters. A computer system was used to record the velocity histories of the three stations with a sampling rate of 512 Hz (512 measurements per second). The field measurements were continuous for about 8 h per day, and computer software was used to pick up the 32-s data for trains passing over this region.

The arrangement of experimental data is explained as follows:

(1) The 32-s vibration $y(t)$ recorded while a train passed this region was obtained first.
(2) Computer software was then used to analyze each 32-s vibration using the fast Fourier transform (FFT) to obtain the frequency-domain vibration data $y(f)$.

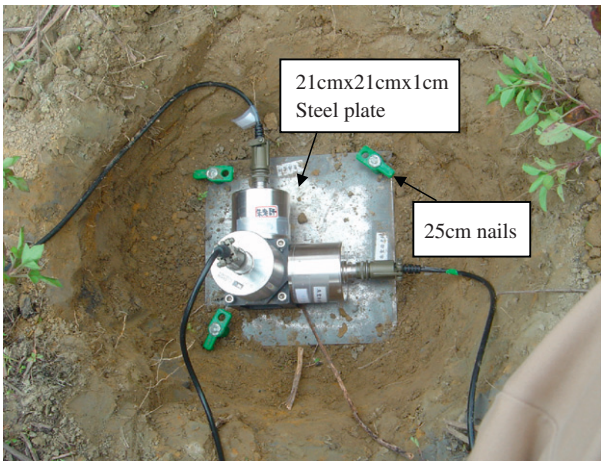

Fig. 3. Installation of velocity meters.

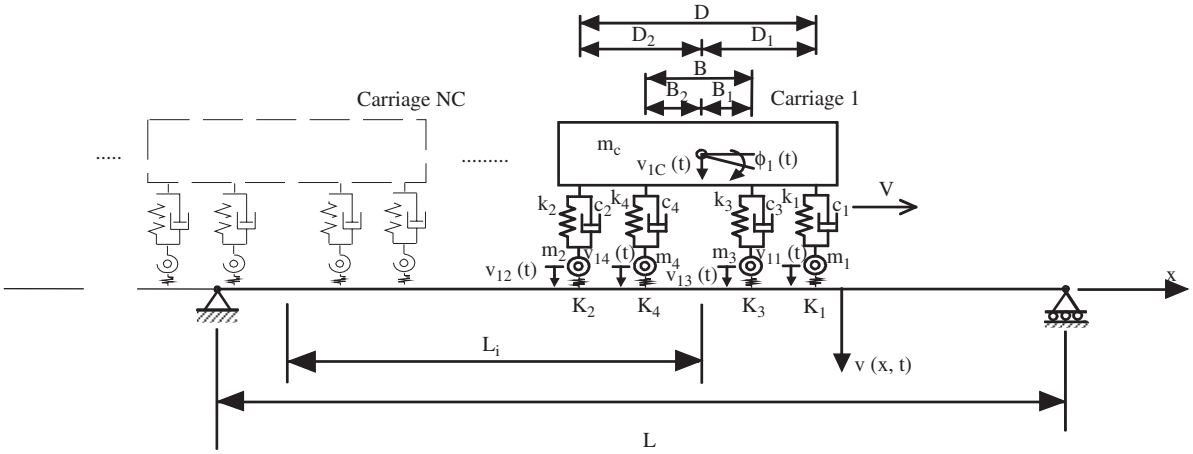

Fig. 4. A series of two-axle vehicles traveling on a simply supported beam.

3.2. Theoretical vibration due to trains moving on a simply supported beam

Theoretical equations modified from Fryba [15] were deduced to perform the parametric study of the vehicle–bridge interaction. In Fig. 4, a series of four-axle vehicles traveling on a simply supported beam was investigated, where each vehicle had six degrees of freedom moving at a uniform speed V on a simply supported bridge of length L. The N matrix equations of motion for N vehicles are:

$$[M]_{6\times6}\begin{Bmatrix}\ddot{\phi}_i(\tau-\tau_i)\\ \ddot{v}_{ic}(\tau-\tau_i)\\ \ddot{v}_{i1}(\tau-\tau_i)\\ \ddot{v}_{i2}(\tau-\tau_i)\\ \ddot{v}_{i3}(\tau-\tau_i)\\ \ddot{v}_{i4}(\tau-\tau_i)\end{Bmatrix}+[C]_{6\times6}\begin{Bmatrix}\dot{\phi}_i(\tau-\tau_i)\\ \dot{v}_{ic}(\tau-\tau_i)\\ \dot{v}_{i1}(\tau-\tau_i)\\ \dot{v}_{i2}(\tau-\tau_i)\\ \dot{v}_{i3}(\tau-\tau_i)\\ \dot{v}_{i4}(\tau-\tau_i)\end{Bmatrix}+[K]_{6\times6}\begin{Bmatrix}\phi_i(\tau-\tau_i)\\ v_{ic}(\tau-\tau_i)\\ v_{i1}(\tau-\tau_i)\\ v_{i2}(\tau-\tau_i)\\ v_{i3}(\tau-\tau_i)\\ v_{i4}(\tau-\tau_i)\end{Bmatrix}=\{F\}_{6\times1},\ i=1,2,3,\ldots,N \quad (6)$$

where

$$[M]_{6\times6}=\begin{bmatrix} I_\phi & 0 & 0 & 0 & 0 & 0\\ 0 & m_c & 0 & 0 & 0 & 0\\ 0 & 0 & m_1 & 0 & 0 & 0\\ 0 & 0 & 0 & m_2 & 0 & 0\\ 0 & 0 & 0 & 0 & m_3 & 0\\ 0 & 0 & 0 & 0 & 0 & m_4 \end{bmatrix}$$

$$[C]_{6\times6}=\begin{bmatrix} D_1^2c_1+D_2^2c_2+B_1^2c_3+B_2^2c_4 & D_1c_1-D_2c_2+B_1c_3-B_2c_4 & -D_1c_1 & D_2c_2 & -B_1c_3 & B_2c_4\\ D_1c_1-D_2c_2+B_1c_3-B_2c_4 & c_1+c_2+c_3+c_4 & -c_1 & -c_2 & -c_3 & -c_4\\ -D_1c_1 & -c_1 & c_1 & 0 & 0 & 0\\ D_2c_2 & -c_2 & 0 & c_2 & 0 & 0\\ -B_1c_3 & -c_3 & 0 & 0 & c_3 & 0\\ B_2c_4 & -c_4 & 0 & 0 & 0 & c_4 \end{bmatrix}$$

$$[K]_{6\times6}=\begin{bmatrix} D_1^2k_1+D_2^2k_2+B_1^2k_3+B_2^2k_4 & D_1k_1-D_2k_2+B_1k_3-B_2k_4 & -D_1k_1 & D_2k_2 & -B_1k_3 & B_2k_4\\ D_1k_1-D_2k_2+B_1k_3-B_2k_4 & k_1+k_2+k_3+k_4 & -k_1 & -k_2 & -k_3 & -k_4\\ -D_1k_1 & -k_1 & k_1 & 0 & 0 & 0\\ D_2k_2 & -k_2 & 0 & k_2 & 0 & 0\\ -B_1k_3 & -k_3 & 0 & 0 & k_3 & 0\\ B_2k_4 & -k_4 & 0 & 0 & 0 & k_4 \end{bmatrix}$$

$$\{F\}_{6\times1}=\begin{Bmatrix} 0\\ 0\\ P_1+P_{31}-\overline{R}_{i1}(\tau-\tau_i)\\ P_2+P_{32}-\overline{R}_{i2}(\tau-\tau_i)\\ P_3+P_{33}-\overline{R}_{i3}(\tau-\tau_i)\\ P_4+P_{34}-\overline{R}_{i4}(\tau-\tau_i) \end{Bmatrix} \tag{7}$$

$P_{31}=m_cg(D-D_1)/2D$, $P_{32}=m_cg(D-D_2)/2D$, $P_{33}=m_cg(B-B_1)/2B$, $P_{34}=m_cg(B-B_2)/2B$, $D=D_1+D_2$, and $B=B_1+B_2$

$$\overline{R}_{ik}(\tau-\tau_i)=K_{ik}[v_{ik}(\tau-\tau_i)-\varepsilon_{ik}v(x_k,\tau-\tau_i)-\overline{r}_{ik}(x_k)],\ k=1,2,3,4 \tag{8}$$

$\tau=\pi Vt/L$, $\tau_i=\pi L_i/L$, L_i is the interval between first and ith four-axle vehicle (Fig. 4), t is time, I_ϕ is the mass moment of vehicle inertia, m_k is the mass of unsprung parts of the vehicle, m_c is the mass of sprung parts of the vehicle, D_k is the horizontal distant between the centroid of a sprung mass and an unsprung mass, c_k is the viscous damping for the four axles, k_k is the spring constant for the four axles, P_k is the weight of wheel k, g is the acceleration of gravity, K_{ik} is the spring constant of the tires, ε_{ik} is zero for wheel k outside the beam domain and is one for wheel k inside the beam domain, and $\overline{r}_{ik}(x_k)$ is the road irregularity at x_k in the z direction. The subscript "k" of symbol is from 1 to 4.

The equation of motion for the simply supported beam is

$$\ddot{q}_{(j)}(\tau)+\frac{2\omega_b L}{\pi V}\dot{q}_{(j)}(\tau)+\frac{4j^4 f_b^2 L^2}{V^2}q_{(j)}(\tau)=\frac{4f_b^2 L^4}{V^2}\sum_{i=1}^{N}\left[\sum_{k=1}^{4}\overline{R}_{ik}(\tau-\tau_i)\sin j(\tau-\tau_i)\right] \tag{9}$$

$$v(x=Vt,t)=\sum_{j=1}^{\infty}q_{(j)}(\tau)\sin j\pi Vt/L \tag{10}$$

$$f_b=\frac{\pi}{2L^2}\left(\frac{EI}{\mu}\right)^{1/2} \tag{11}$$

where ω_b (rad/s) is the circular frequency of beam damping, f_b is the first natural frequency (Hz) of the beam, E is the Young's modulus of the beam, I is the constant moment of inertia of the beam cross section, and μ is the mass per unit length of the beam.

3.3. Theoretical vibration due to trainloads moving on a semi-infinite profile

This section generates the half-space vibrations induced by multi-moving loads using the vibration solution of a single moving load [16]. First, assume that the load moves along the X-axis, Y-axis is perpendicular to the load path (X-axis) and Z-axis is the vertical direction (parallel to the load direction). The displacement vector of a moving load on the half-space is defined as $\mathbf{W}(X, Y, Z, t)$ for $t \geqslant 0$ and as zero for $t<0$, where t is the time. The summation procedure of Eq. (12) can be used to obtain the total transient displacement $W^A_{\text{Total}}(X_A, Y_A, Z_A, t)$ at point A when there is a multi-moving load on the half-space:

$$\mathbf{W}^A_{\text{Total}}(X_A, Y_A, Z_A, t)=\sum_{i=0}^{N}\mathbf{W}(X_A, Y_A, Z_A, t-L_i/V) \tag{12}$$

where L_i is the distance between the first and the ith loads and V is the train speed.

4. Vibration behavior of a train moving on a bridge

First, the theoretical solution of Section 3.2 was used to investigate the vibration behavior of trains moving on a simply supported bridge. The bridge length was 30 m with the input data of $E=2\times10^8$ kPa, $I=3\,\text{m}^4$, and $\mu=40$ t/m. The first natural frequency of this bridge is 6.76 Hz, similar to the measured natural frequency of the high-speed train bridge in Taiwan. The HSR-700T train, as shown in Fig. 2(b), was used with the input

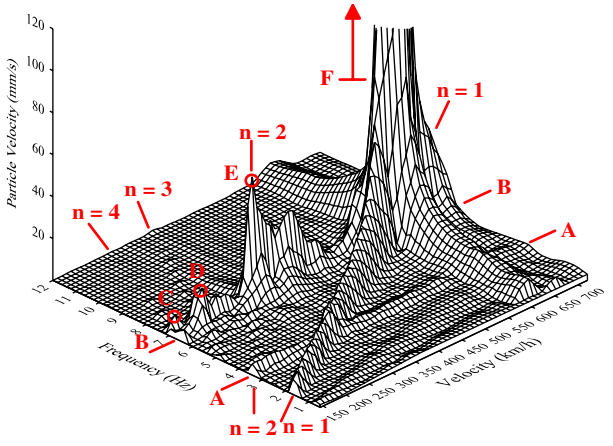

Fig. 5. Wire-frame figure of the vertical particle velocity at the beam center generated from Eqs. (6) to (12) for the HSR-700T high-speed train moving on a bridge.

data of $K_k = 4 \times 10^5$ kN/m, $k_k = 30000$ kN/m, $c_k = 10$ kN-s/m, $m_k = 0.1$ t, and $m_c = 250$ t. The subscript "k" of symbol is from 1 to 4. This large carriage mass was used to obtain a large ratio (25%) of the train mass to the bridge mass, so that the train–bridge interaction can be significant. The Newmark method was used to solve this problem with the Newmark constants of 0.5 and 0.25. The time step length was 5e−7 s.

Fig. 5 shows the wire-frame figure of the vertical particle velocity at the beam center generated from Eqs. (6) to (12) under the above condition. This figure, obtained from the theoretical solution, indicates the following features:

(1) The particle velocities along straight lines ($f_n = nV/L$ for $n = 1,2,3$, and 4) are apparently large, which indicates that the trainload frequencies of nV/L are dominant. When n equals one, the particle velocities are much larger than those of others and the wire-frame figure reveals that the vibration magnitude is approximately linearly proportional to the train speed before the first dominant-frequency approaches the first bridge natural frequency.
(2) When the dominant frequencies equal the first bridge natural frequency (6.76 Hz), the vibrations are large (B–B line). This condition can be clearly seen at points C, D, E, and F as shown in Fig. 5, where points C, D, E, and F indicate the resonance of the first bridge natural frequency with the fourth, third, second, and first trainload dominant frequencies, respectively. For the resonance with the first trainload dominant (point F), the vibration increases significantly, so this condition must be avoided. Usually, the first bridge vertical natural frequency is considerably high, so the resonance will occur at a very fast train speed, which is often much faster than the operational train speed. However, for the resonance with second or higher trainload dominant frequencies, the probability is high, since the trainload frequency of the operational train speed may coincide with the second or higher dominant frequencies.
(3) The vertical natural frequency of the train carriage is 3.5 Hz, which can be clearly seen in Fig. 5 (line A–A). Resonance will not be invoked when this frequency approaches the trainload dominant frequencies because the carriage is moving at the same speed as the trainload, so the trainload will not affect the stiffeners and dampers of carriages.

Experimental results were then used to investigate the characteristics of the trainload. The field experiment was performed in southern Taiwan with a modified HSR-700T high-speed train as shown in Fig. 2(b). The train speeds ranged from 160 to 315 km/h during the field experiment. The bridge is a series of simply supported beams with a span of 30 m as shown in Fig. 6. Using the train speeds and frequencies as the two horizontal axes and the frequency-domain vibrations as the vertical axis, wire-frame figures can be obtained. Fig. 7 shows the wire-frame figures of the railway (X) and vertical (Z) direction vibrations measured at 200 m from the bridge. Because the carriage interval L is constant for the HSR-700T high-speed train, the dominant frequency ($f_n = nV/L$) for a certain n is linearly proportion to the train speed V, so the vibration along this line should be large. This condition can be clearly observed in the two wire-frame figures, in which the vibration

Fig. 6. Field experiments for measuring train-induced vibrations on simply supported bridges.

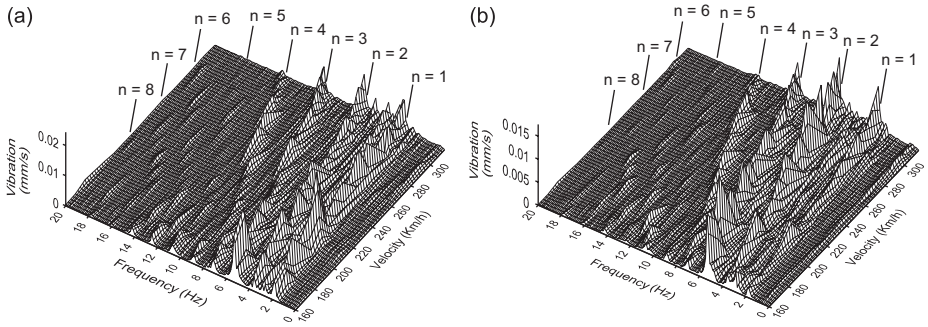

Fig. 7. Wire-frame figures of X and Z vibrations for the HSR-700T high-speed train moving on multi-simply supported bridges measured at 200 m from the bridge. (a) X-vibration (railway direction), (b) Z-vibration (vertical direction).

Fig. 8. Experiment location of the Taipei MRT train moving on a bridge.

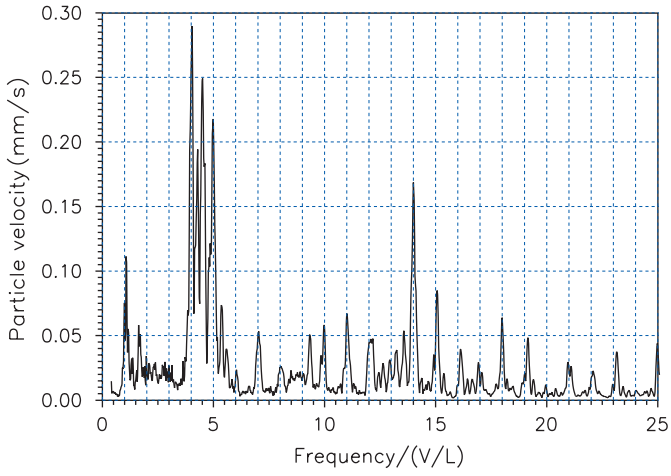

Fig. 9. Particle velocity changing with frequency measured near the bridge pier for the Taipei MRT train moving on bridges.

along the dominant-frequency lines (nV/L for $n = 1$, 2, 3, 4, 6, and 7) is apparently large. Thus, although the trainload is in the vertical direction, the train-induced ground vibration is still dominated by the trainload frequency in other directions.

Another field experiment used in this section is the Taipei MRT train moving on a bridge as shown in Fig. 8. The Taipei MRT train as shown in Fig. 2(c) has only two wheel axes in a carriage with a relatively short carriage length of 13.78 m and fewer (four) carriages. The interval between the two wheel axes is 10 m. The elevated railway is a series of simply supported beams with a span of 25 m and the first natural frequency of the bridge in vertical direction is about 4.5 Hz. Fig. 9 shows the experimental results in the frequency domain of this train moving on the bridge at a train speed of 65 km/h. This result indicates that the particle velocities are large at the trainload dominant frequencies nV/L. In addition, the large vibration near the normalized frequency of 5 is due to the trainload dominant frequencies approaching the first bridge vertical natural frequency. Other ambient vibrations, especially from the moving vehicles near the measured location, are much smaller than that from the MRT train.

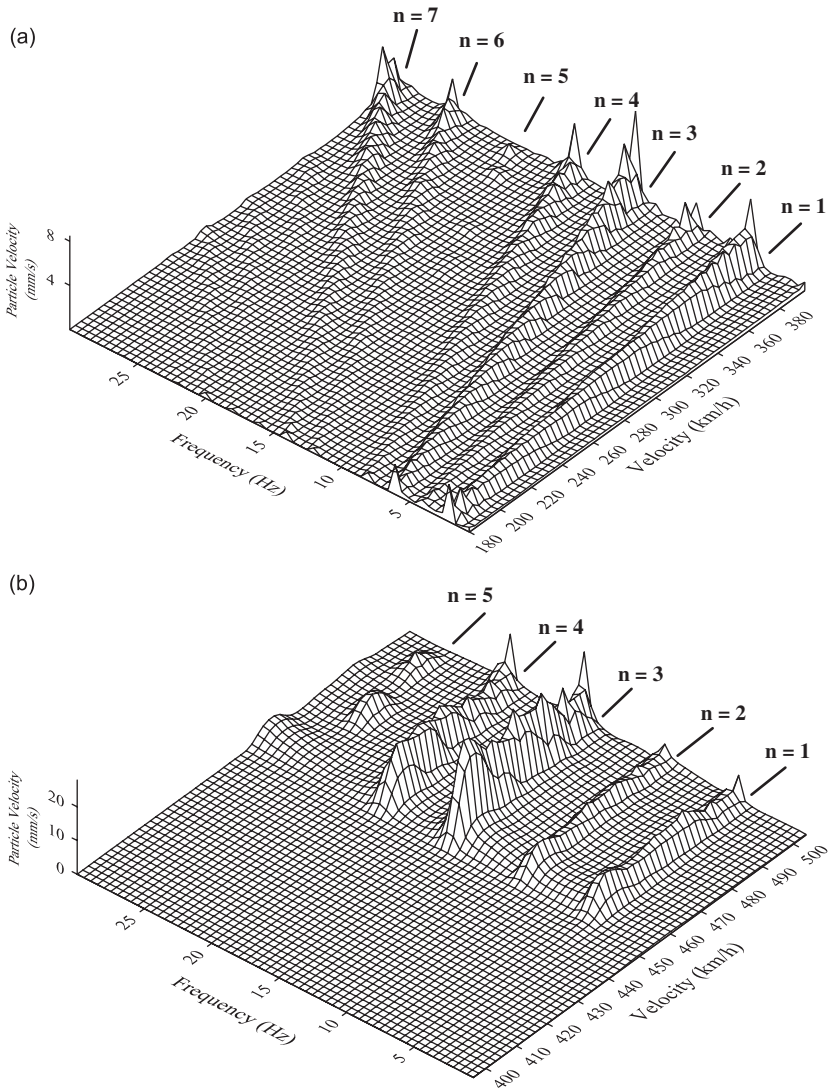

Fig. 10. Wire-frame figures of the vertical particle velocity from Eq. (1) under the trainloads of the HSR-700T high-speed train as shown in Fig. 2(b). (a) Subsonic speed (Measured location is 2 m from the rail), (b) supersonic speed (Measured location is 100 m from the rail).

5. Vibration behavior of trains moving on the ground

First, the theoretical solution of Section 3.3 was used to investigate the vibration behavior of trains moving on the ground. Fig. 10 shows the wire-frame figure of the vertical particle velocity generated from Eq. (12) under the trainloads of the HSR-700T high-speed train at subsonic and supersonic speeds. This figure, obtained from the theoretical solution, indicates the following features:

(1) The particle velocities along straight lines ($f_n = nV/L$ for $n = 1$, 2, 3, 4, 6, and 7) are apparently large, which indicates that the trainload frequencies of nV/L are dominant. When n equals five, the particle velocities are much smaller. This is consistent with the near zero influence factor in Eq. (3) and Fig. 1(b) for $n = 5$.
(2) When the train speed is over the soil Rayleigh wave speed, the vibrations increase considerably. The vibration dominant frequencies are clearly equal to nV/L, which are the same as those of the train moving at subsonic speeds.
(3) For trains moving at subsonic speeds, the wire-frame figure reveals that the vibration magnitude is approximately linearly proportional to the train speed. For trains at supersonic speeds, this condition may

Fig. 11. Location of the experiment near a complicated site with an embankment, a bridge, and a tunnel.

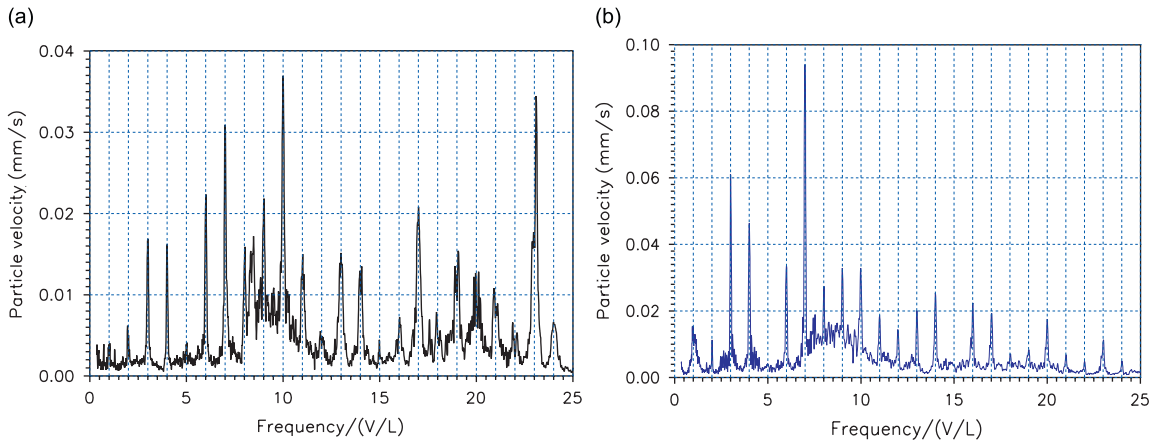

Fig. 12. Experimental results of the HSR-700T high-speed train moving on the embankment and in the tunnel. (a) 40 m near the tunnel entrance, (b) at the embankment edge and 15 m from the railway.

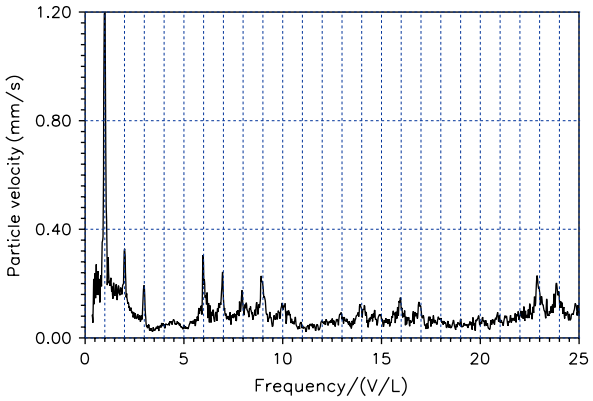

Fig. 13. Experimental results for the Taiwan railway train moving on the ground (5 m from the railway).

not be true, but the large vibration is difficult to attenuate. Fig. 10(b) shows that the vibration of a train at supersonic speed at 100 m from the railway is much larger than that of a train at subsonic speed at 2 m from the railway.

The field experiments used in this section contain the HSR-700T high-speed train moving on an embankment and in a tunnel in central Taiwan and the railway train moving on the ground in southern Taiwan. Fig. 11 shows one of the measurement locations, which is a complicated site that includes a tunnel, an embankment, and a bridge. Figs. 12 and 13 show the experimental results in the frequency domain of the HSR-700T high-speed train moving on the embankment and in the tunnel (train speed of 270 km/h) and Taiwan railway train moving on the ground (train speed of 110 km/h). These results all indicate that the particle velocities are large at the trainload dominant frequencies nV/L. Additionally, the particle velocities at several dominant frequencies, such as $n = 5$ and 15 for HSR-700T high-speed train and $n = 4$ and 5 for Taiwan railway train, disappear, which is consistent with the near zero influence factor in Figs. 1(a) and (b) obtained from Eq. (3).

After the train-induced wave transfers from a complicated site with soil or tunnels, the magnitude of the measured vibration at the trainload dominant frequencies may be different from the theoretical result, as shown in Fig. 1(b). However, almost all the vibration peaks are still located at the trainload dominant frequencies, which mean that the trainload vibration is the most important one and the vibration from other sources, such as carriage natural frequencies and vehicle engines, are minor.

6. Conclusions

A moving train often produces significant ground vibrations, which may cause significant environmental problems. Thus, understanding the behavior of vibrations induced by moving trains is becoming increasingly important. This paper investigates the characteristics of the ground vibrations induced by moving trains using field measurements and theoretical solutions. Both experimental and theoretical results indicate that the particle velocities are large at the trainload dominant frequencies nV/L, which means that the trainload vibration is the most important one and the vibration from other sources, such as carriage natural frequencies and vehicle engines, are minor. This condition is true for trains moving on the ground, an embankment, bridges, or in tunnels whether moving at subsonic or supersonic train speeds. For the high-frequency range ($f > 25V/L$), the dominant frequencies of train-induced vibrations were not mentioned in this paper, and this problem should be the topic of sound noise that often is generated from the contact of wheels and rails.

When the trainload dominant frequencies equal the bridge natural frequency, the vibration is large. Especially for the resonance of the first trainload dominant frequency and the first bridge natural frequency, the vibration increases significantly. Because the trainload dominant frequencies only depend on the train speed over the carriage length, the train can run at a reasonable operational speed while avoiding resonance.

This study also indicates that resonance will not be invoked when the natural frequencies of the train carriage approach the trainload dominant frequencies. Thus, the ground vibrations induced by the dampers and springs of the carriage are not serious.

Acknowledgment

This study was supported by the National Science Council, Republic of China, under Contract no. NSC89-2218-E-006-019.

References

[1] J.Z. Li, M.B. Su, The resonant vibration for a simply supported girder bridge under high-speed trains, *Journal of Sound and Vibration* 224 (5) (1999) 897–915.
[2] J.F. Wang, C.C. Lin, B.L. Chen, Vibration suppression for high-speed railway bridges using tuned mass dampers, *International Journal of Solids and Structures* 40 (2) (2003) 465–491.
[3] Y.B. Yang, J.D. Yau, L.C. Hsu, Vibration of simple beams due to trains moving at high speeds, *Engineering Structures* 19 (11) (1997) 936–944.
[4] S.H. Ju, Three-dimensional analyses of wave barriers for reduction of train-induced vibrations, *Journal of Geotechnical and Geoenvironmental Engineering* 130 (7) (2004) 740–748.
[5] Y.S. Wu, Y.B. Yang, Steady-state response and riding comfort of trains moving over a series of simply supported bridges, *Engineering Structures* 25 (2) (2003) 251–265.
[6] H. Xia, N. Zhang, W.W. Guo, Analysis of resonance mechanism and conditions of train–bridge system, *Journal of Sound and Vibration* 297 (3–5) (2006) 810–822.
[7] S.H. Ju, H.T. Lin, Numerical investigation of a steel arch bridge and interaction with high-speed trains, *Engineering Structures* 25 (2) (2003) 241–250.
[8] S.H. Ju, H.T. Lin, Resonance characteristics of high-speed trains passing simply supported bridges, *Journal of Sound and Vibration* 267 (5) (2003) 1127–1141.
[9] J.D. Yau, Y.B. Yang, A wideband MTMD system for reducing the dynamic response of continuous truss bridges to moving train loads, *Engineering Structures* 26 (12) (2004) 1795–1807.
[10] S.H. Ju, Finite element analysis of structure-borne vibration from high-speed train, *Soil Dynamic and Earthquake Engineering* 27 (3) (2007) 259–273.
[11] Y.B. Yang, C.L. Lin, J.D. Yau, D.W. Chang, Mechanism of resonance and cancellation for train-induced vibrations on bridges with elastic bearings, *Journal of Sound and Vibration* 269 (1–2) (2004) 345–360.
[12] J.D. Yau, Y.B. Yang, Vertical accelerations of simple beams due to successive loads traveling at resonant speeds, *Journal of Sound and Vibration* 289 (1–2) (2006) 210–228.
[13] S.H. Ju, H.T. Lin, Analysis of train-induced vibrations and vibration reduction schemes above and below critical Rayleigh speeds by finite element method, *Soil Dynamic and Earthquake Engineering* 24 (12) (2004) 993–1002.
[14] S.H. Ju, H.T. Lin, T.K. Chen, Studying characteristics of train-induced ground vibrations adjacent to an elevated railway by field experiments, *Journal of Geotechnical and Geoenvironmental Engineering* 133 (10) (2007) 1302–1307.
[15] L. Fryba, *Vibration of Solids and Structures Under Moving Load*, Thomas Telford, London, 1999.
[16] G. Lykotrafitis, H.G. Georgiadis, The three-dimensional steady-state thermo-elastodynamic problem of moving sources over a half space, *International Journal of Solids and Structures* 40 (4) (2003) 899–940.